Reaction Dynamics of Phenyl Radicals (C_6H_5, X^2A') with Methylacetylene ($CH_3CCH(X^1A_1)$), Allene ($H_2CCCH_2(X^1A_1)$), and Their D4-Isotopomers

Xibin Gu, Fangtong Zhang, Ying Guo, and Ralf I. Kaiser*

Department of Chemistry, University of Hawaii at Manoa, Honolulu, Hawaii 96822

Received: May 17, 2007; In Final Form: August 24, 2007

Crossed molecular beam experiments were utilized to untangle the reaction dynamics to form 1-phenylmethylacetylene [$CH_3CCC_6H_5$] and 1-phenylallene [$C_6H_5HCCCH_2$] in the reactions of phenyl radicals with methylacetylene and allene, respectively, over a range of collision energies from 91.4 to 161.1 kJ mol^{-1}. Both reactions proceed via indirect scattering dynamics and are initiated by an addition of the phenyl radical to the terminal carbon atom of the methylacetylene and allene reactants to form short-lived doublet C_9H_9 collision complexes $CH_3CCHC_6H_5$ and $C_6H_5H_2CCCH_2$. Studies with isotopically labeled reactants and the information on the energetics of the reactions depict that the energy randomization in the decomposing intermediates is incomplete. The collision complexes undergo atomic hydrogen losses via tight exit transition states leading to 1-phenylmethylacetylene [$CH_3CCC_6H_5$] and 1-phenylallene [$C_6H_5HCCCH_2$]. The possible role of both C_9H_8 isomers as precursors to PAHs in combustion flames and in the chemistry of circumstellar envelopes of dying carbon stars is discussed.

1. Introduction

Chemical reaction networks modeling the formation of polycyclic aromatic hydrocarbons (PAHs) in combustion flames[1,2] and in carbon-rich circumstellar envelopes[3] imply that the phenyl radical, C_6H_5, in its $^2A_1$ electronic ground state presents one of the most important transient species to initiate the formation of PAHs. All networks concur that phenyl radical reactions with unsaturated hydrocarbon molecules such as (substituted) acetylenes, olefines, and aromatic molecules initiate the PAH synthesis via an addition of the radical center of the phenyl radical to the π electronic system of the unsaturated co-reactant forming doublet radical intermediates. Depending on the temperature and pressure conditions, theoretical investigations coupled with kinetics studies of these reactions suggested that the intermediates either decompose back to the reactants, fragment predominantly via atomic hydrogen loss pathways, isomerize prior to their decomposition, and/or are stabilized at higher pressures if the life time of the intermediate is longer than the time scale necessary to divert the internal energy of the complexes via a third body collision.[4]

During the last years, the reactions of phenyl radicals with methylacetylene ($CH_3CCH(X^1A_1)$) and allene (H_2CCCH_2-(X^1A_1)) have received considerable attention both from the theoretical and experimental points of view. This was triggered due to the potential involvement of the formation of the indene molecule (C_9H_8) in combustion flames and in circumstellar envelopes of carbon stars (Figure 1). Peeters et al. and Bettinger et al. investigated theoretically the rate coefficients and product distributions of the reactions of phenyl radicals with methylacetylene[5,6] and allene[7] over extended temperature and pressure ranges up to 4000 K and 100 atm. The authors suggested that indene should be the dominant product at temperatures up to 500 K and pressures lower than about 10^{-7} Torr. At combustion temperatures (800−2000 K), the reaction was predicted to give about 30% phenylallene ($PhCHCCH_2$) + H, 30% phenylacetylene (PhCCH) + methyl (CH_3), 15% phenylmethylacetylene ($PhCCCH_3$) + H, and 20% benzene + 2-propynyl; in particular, the abstraction pathway leading to benzene + 2-propynyl was predicted to increase from 20% at 800 K to 50% at 2000 K. Considering the C_9H_8 isomers, at higher temperatures (3000−4000 K), indene was found to be only a small fraction of all the C_9H_8 isomers formed; instead, 1-phenylmethylacetylene and 1-phenylallene were predicted to be the dominating C_9H_8 isomers (Figure 1). A recent crossed beam study of the phenyl radical reaction with methylacetylene at a collision energy of 140 kJ mol^{-1} suggested the synthesis of 1-phenylmethylacetylene under single collision conditions.[8,9] Considering the phenyl plus allene reaction, the authors concluded that within the limits of a complete energy randomization, at low temperatures (<1000 K) the dominant products are indene plus atomic hydrogen, while at high temperatures the hydrogen abstraction channel leading to benzene + 2-propynyl might become the most important channel, analogously to what predicted for the methylacetylene reaction. Other important products are predicted to be $PhCH_2 + C_2H_2$ (up to 18%), $PhCH_2CCH$ + H (10−14%), $PhCHCCH_2$ (5−10%), and PhCCH + CH_3 (5%).

Although Peeters et al. and Lin et al. carried out detailed computational[5,6] and kinetics studies[4] on the reactions of phenyl radicals with methylacetylene and allene, various aspects of these systems have not been resolved to date. First, it is important to compare these computations with crossed beam experiments over a wide range of collision energies; recall that the current computations are conducted within the assumption of a complete energy randomization. However, recent crossed beam experiments of, for example, carbon atoms with benzene[10]- and 1,2-butadiene,[11] have showed that under single collision conditions, the energy randomization is not always complete, and a non-statistical outcome of the reaction can be observed, too. Second, it is crucial to see to what extent a potential hydrogen atom loss in the crossed beam reaction originated from the C_3H_4 isomer(s) or from the phenyl radical itself. Third, by

* To whom correspondence should be addressed. E-mail: ralfk@hawaii.edu.

10.1021/jp0738255 CCC: $37.00
Published on Web 10/13/2007

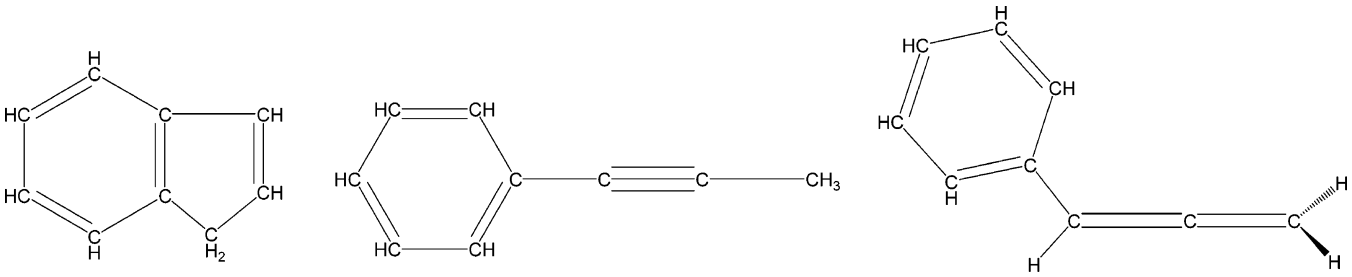

indene 1-phenylmethylacetylene 1-phenylallene

Figure 1. Molecular structures of three C_9H_8 isomers that can be formed in the reactions of phenyl radicals with methylacetylene and allene.

conducting the crossed beam reactions over a wide range of collision energies, it is possible to derive the collision-energy-dependent life time of the decomposing reaction; this will also shed light of the question to what extent osculating complexes are involved in the chemical dynamics of the title reactions; note that the life time of the intermediate(s) can influence dramatically the role of potential hydrogen migrations and hence the final reaction products, i.e., indene (its formation requires successive isomerization steps) versus the formation of 1-phenylmethylacetylene and 1-phenylallene isomers where hydrogen migrations are not necessary. This is also important to correlate the crossed beam reactions with those conditions prevailing in combustion flames.

2. Experimental Section

The experiments were conducted under single collision conditions in a crossed molecular beam machine at The University of Hawai'i.[12] Briefly, a pulsed supersonic beam of phenyl radicals was generated by flash pyrolysis of a nitroso benzene precursor (C_6H_5NO, Aldrich) at seeding fractions of less than 0.1% in the primary source chamber employing a modified Chen source;[13] this unit was coupled to a piezoelectric pulsed valve operated at 200 Hz.[14] Helium gas (3040 Torr) (Matheson, 99.9999%) was introduced into a stainless steel reservoir; the latter kept the nitroso benzene sample at a temperature of 283 K. The mixture was expanded at a backing pressure of 920 Torr through a resistively heated silicon carbide tube; the temperature of the tube was estimated to be about 1200−1500 K. At these experimental conditions, the decomposition of the nitroso benzene molecule to form nitrogen monoxide and the phenyl radical was *quantitative*. Compared to a previous design of this phenyl radical source,[9] we obtained enhanced phenyl radical number densities by 1 order of magnitude, a higher repetition rate of the pulsed valve (200 vs 60 Hz), and a significantly extended operation time of the silicon carbide nozzle before clogging (2 weeks vs 1 day). After passing a skimmer, a four-slot chopper wheel selected a part of the phenyl radical beam; the peak velocities and speed ratios of the segments of the beams crossing in the interaction region are compiled in Table 1. This phenyl radical beam intersected pulsed methylacetylene [$CH_3CCH(X^1A_1)$, Linde; 99.8%], allene [H_2CCCH_2 (X^1A_1), Aldrich; 99.5%], D4-allene [D_2CCCD_2; CDN; 99% + D], and D4-methylacetylene [CD_3CCD; CDN; 99% + D] beams released by a second pulsed valve at a pressure of 550 Torr under well-defined collision energies (Table 1). The angular divergences of the primary and secondary beams were determined to be 2.8 and 2.5°, respectively. Note that the D4-methylacetylene and D4-allene experiment were conducted to elucidate on the position of the hydrogen/deuterium atom loss, i.e., an emission from the methylacetylene/allene molecule versus the phenyl moiety.

TABLE 1: Peak Velocities (v_p), Speed Ratios (S), Center-of-Mass Angles (Θ_{CM}), and the Collision Energies of the Phenyl Radical as Well as the Reactants (E_c)[a]

beam	v_p, ms^{-1}	S	E_c, kJ mol^{-1}	CM
$CH_3CCH(X^1A_1)$	840 ± 3	12.5 ± 1.0	−	−
$C_6H_5(X^2A_1)$	2498 ± 64	4.8 ± 1.0	91.4 ± 4.3	9.9 ± 0.3
$CH_3CCH(X^1A_1)$	840 ± 3	12.5 ± 1.0	−	−
$C_6H_5(X^2A_1)$	3396 ± 16	5.6 ± 0.5	161.1 ± 1.5	7.3 ± 0.1
$CD_3CCDX^1A_1)$	830 ± 5	12.5 ± 1.0	−	−
$C_6H_5(X^2A_1)$	3037 ± 71	5.7 ± 0.2	139.0 ± 6.2	9.0 ± 0.2
$H_2CCCH_2(X^1A_1)$	840 ± 3	12.5 ± 1.0	−	−
$C_6H_5(X^2A_1)$	2517 ± 45	4.3 ± 0.1	92.7 ± 3.1	9.8 ± 0.2
$H_2CCCH_2(X^1A_1)$	840 ± 3	12.5 ± 1.0	−	−
$C_6H_5(X^2A_1)$	2866 ± 40	5.7 ± 1.2	117.4 ± 3.1	8.7 ± 0.1
$H_2CCCH_2(X^1A_1)$	840 ± 3	12.5 ± 1.0	−	−
$C_6H_5(X^2A_1)$	3054 ± 70	7.1 ± 0.6	132.1 ± 5.8	8.1 ± 0.2
$D_2CCCD_2(X^1A_1)$	830 ± 5	12.5 ± 1.0	−	−
$C_6H_5(X^2A_1)$	2956 ± 71	5.7 ± 0.2	132.2 ± 6.0	9.2 ± 0.2

[a] To obtain a crossing of the phenyl radical beam with identical segments of the secondary beam in the experiments, the delay times between both pulsed valves had to be adjusted from experiment to experiment to account for the distinct velocities of the primary beam.

The reactively scattered products were probed using a quadrupole mass spectrometric detector in the time-of-flight (TOF) mode after electron-impact ionization of the molecules. The detector could be rotated within the plane defined by the primary and the secondary reactant beams to take angular resolved TOF spectra. By integrating the TOF spectra at the laboratory angles, the laboratory angular distribution, which depicted the integrated signal intensity of an ion of distinct m/z versus the laboratory angle, could be obtained. Information on the chemical dynamics was gained by fitting these TOF spectra and the angular distribution in the laboratory frame (LAB) using a forward-convolution routine.[15] This approach initially assumed an angular distribution $T(\theta)$ and a translational energy distribution $P(E_T)$ in the center-of-mass reference frame (CM). It should be stressed that this fitting route accounts for the transformation Jacobian and averages over the apparatus and beam functions such as the velocity distribution as expressed via the speed ratio and the angular divergence. Because the previous kinetic studies of phenyl radical reactions with allene and methylacetylene showed the existence of a threshold energy to reaction, E_o,[5,7] we included an energy-dependent cross section, $\sigma(E_C) \approx [1 - E_o/E_C]$, via the line-of-center model with the collision energy E_C for $E_C \geq E_o$ in the fitting routine.[16] TOF spectra and the laboratory angular distribution were then calculated from these center-of-mass functions. Due to the low signal counts, we had to accumulate up to 6×10^6 TOF spectra to obtain a reasonable

signal-to-noise ratio of the reactively scattered species. This limited us to conduct the experiments with the D4-methylacetylene and D4-allene reactants only at the corresponding center-of-mass angles.

3. Results

3.1. Laboratory Data. In both the phenyl−allene and phenyl−methylacetylene reactions, reactive scattering signal was recorded at mass-to-charge ratios from $m/z = 116$ ($C_9H_8^+$) (Figure 2) down to $m/z = 112$ ($C_9H_4^+$). It is important to stress that for each reaction, the TOF spectra recorded at lower m/z ratios showed identical pattern and could be fit with identical center-of-mass functions as $m/z = 116$. Consequently, signal at these ions originated from dissociative ionization of the parent molecule in the electron impact ionizer of the detector; further, we can conclude that within the mass range of $m/z = 116-112$ in the reactions of the phenyl radical with methylacetylene and allene, only the phenyl versus atomic hydrogen pathways were open. We also investigated a potential methyl group (CH_3) loss and monitored signal at $m/z = 102$ ($C_8H_6^+$); however, the TOFs recorded are, after scaling, superimposable to those taken at $m/z = 116$. Consequently, the methyl group elimination channel is closed. We acknowledge that compared to the atomic hydrogen elimination pathway, the methyl group loss is kinematically unfavorable. However, considering the data accumulation time at $m/z = 116$ vs 102 and the signal-to-noise of our experiments, we can derive upper fractions of the methyl loss pathway of about 8%. Finally, it should be noted that we also observed signal at $m/z = 117$. Due to the strength of the ion counts of about 10% compared to $m/z = 116$, the fact that we observed signal at $m/z = 117$ at various laboratory angles, and the identical shape of the TOFs of $m/z = 116$ and $m/z = 117$, we can conclude that signal at $m/z = 117$ originated from $^{13}CC_8H_8^+$, but not from any $C_9H_9^+$ adduct. Figure 3 compiles the LAB distributions of the ion counts at $m/z = 116$. It is evident that all LAB distributions are very narrow and are spread only over about 14° in the scattering plane. In addition, all LAB distributions are slightly forward peaked with respect to the corresponding center-of-mass angles. It should be noted that we also attempted to investigate potential hydrogen abstraction pathways to form $C_6H_6 + C_3H_3$. However, elastically scattered ^{13}C-phenyl radicals $^{13}CC_5H_5$ ($m/z = 78$) which account for about 6% of the phenyl radicals in the beam lead to strong background at $m/z = 78$. Therefore, we conducted crossed beam reactions of phenyl radicals with D4-allene and D4-methylacetylene. Here, no background at $m/z = 79$ is present (C_6H_5D). However, we were not able to detect any reactive scattering product of the D abstraction channel. We recognize that compared to the atomic hydrogen loss channel, this pathway is kinematically unfavorable. However, accounting for the data accumulation times, we can derive upper limits of about 10−15% of the D abstraction pathway.

Finally, we collected additional information on the position of the hydrogen loss and aimed to unravel to what extent the hydrogen atom is lost from the phenyl group and/or from the allene/methylacetylene reactant. Therefore, we conducted experiments of phenyl radicals (C_6H_5) with D4-methylacetylene and D4-allene (both C_3D_4). In case of an atomic hydrogen loss, signal should be observable at $m/z = 120$ ($C_9H_4D_4^+$); if a deuterium atom elimination is present, we should be able to monitor ion counts at $m/z = 119$ ($C_9H_5D_3^+$). Note that, in principle, $m/z = 119$ can also originate from fragmentation of $m/z = 120$. When we carried out the experiments, we observed signal at $m/z = 119$ for the reactions of phenyl radicals with D4-allene and methylacetylene (Figure 4). Within the signal-to-noise limit, we could not detect any ion counts at $m/z = 120$. This leads us to conclude that only the deuterium atom is being released. Consequently, in the reactions of phenyl with allene and methylacetylene, the hydrogen atom is emitted from the C_3H_4 reactants. Since we used perdeuterated reactants, we could only scan 10^6 shots at the corresponding center-of-mass angles. Therefore, the signal-to-noise of these data as presented in Figure 4 is lower that in the corresponding reactions with methylacetylene and allene (Figure 2). Recall that a preliminary study of the reaction of phenyl with methylacetylene utilized a D3-methylacetylene reactant (CD_3CCH);[9] these experiments showed that the hydrogen atom is only ejected from the acetylenic carbon atom.

3.2. Center of Mass Translational Energy, P(E_T)s, and Angular Distributions, T(θ)s. For both the phenyl−methylacetylene and phenyl−allene reactions, the TOF data (Figure 2) and LAB distributions (Figure 3) could be fit with a single reaction channel leading to a product of the generic formula C_9H_8 plus atomic hydrogen. The corresponding center-of-mass functions are shown in Figure 5. Best fits of the translational energy distributions, P(E_T)s, could be obtained with distributions extending to maximum translational energy releases, E_{max}, of 97 ± 8 and 165 ± 8 kJ mol^{-1} (methylacetylene reaction; lower and higher collision energies, respectively) as well as 109 ± 6, 133 ± 7, and 148 ± 5 kJ mol^{-1} (allene reaction, lowest, medium, and highest collision energy, respectively). The high-energy cutoffs, i.e., the sum of the absolute of the reaction energy plus the collision energy, allow us to calculate the corresponding reaction energies. In the phenyl−allene system, an exoergicity of 14 ± 8 kJ mol^{-1} was obtained. In the case of the methylacetylene−phenyl reaction, it is difficult to pin down if the reaction is slightly exoergic to a maximum of 13 kJ mol^{-1} or, within the error limits, even slightly endoergic by a few kJ mol^{-1}. All P(E_T)s are very broad and show pronounced distribution maxima in the range of 30−60 kJ mol^{-1}, i.e., peaks well away from zero translational energy. As the collision energy increases, the peak positions move toward higher energies (Figure 5). This off-zero peaking suggests that the reactions of the phenyl radicals with methylacetylene and allene likely involve tight exit transition states.[17]

The center-of-mass angular distributions help to gain additional information on the reaction dynamics. In both the C_6H_5/CH_3CCH and C_6H_5/H_2CCCH_2 systems, the angular flux distributions are asymmetric around 90° and show intensity over the complete angular range; note that within the error limits, the data of the phenyl−methylacetylene reaction at collision energy of 161.1 kJ mol^{-1} could also be fit with intensity covering 0 to 155°. As shown in Figure 5, a pronounced flux in the forward hemisphere (with respect to the phenyl radical beam) is evident for each distribution. Also, as the collision energy rises, the T(θ)s are increasingly forward peaked. In case of the phenyl−allene system, for instance, the ratios at the poles, T(180°)/T(0°), changes from 0.55 ± 0.10 via 0.30 ± 0.08 to 0.17 ± 0.05 from the highest to the lowest collision energy. These data suggest that the reactions follow indirect scattering dynamics and that the life-times of the C_9H_9 intermediate(s) are lower than the rotational period of the reaction intermediate(s) at all collision energies. In addition, the enhanced asymmetry and pronounced forward peaking, which goes hand in hand with rising collision energies, indicate the existence of an osculating C_9H_9 complex[18] in each system. Here, the life time of the reaction intermediate decreases as the collision energy is enhanced. Note that at the highest collision energy of the phenyl−methylacetylene reaction,

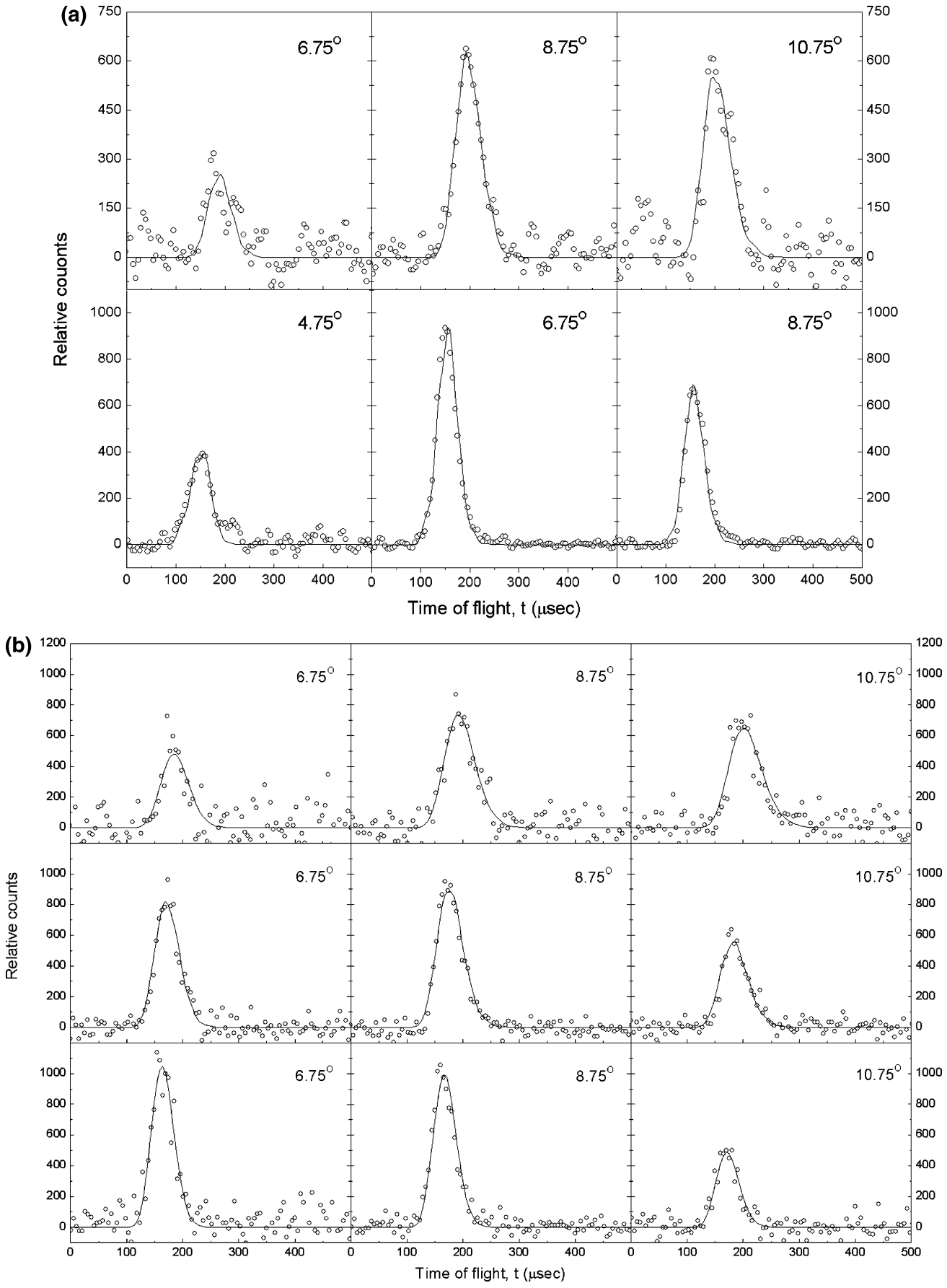

Figure 2. (a) Selected time of flight data recorded at mass-to-charge (m/z) of 116 ($C_9H_8^+$) in the reaction of phenyl radicals with methylacetylene for two collision energies of 91.4 (upper row) and 161.1 kJ mol^{-1} (lower row). The open circles are the experimental data, and the solid lines are the fits. (b) Selected time-of-flight data recorded at m/z 116 ($C_9H_8^+$) in the reaction of phenyl radicals with allene for three collision energies of 92.7 (upper row), 117.4 (center row), and 132.1 kJ mol^{-1} (lower row). The open circles are the experimental data, and the solid lines are the fits.

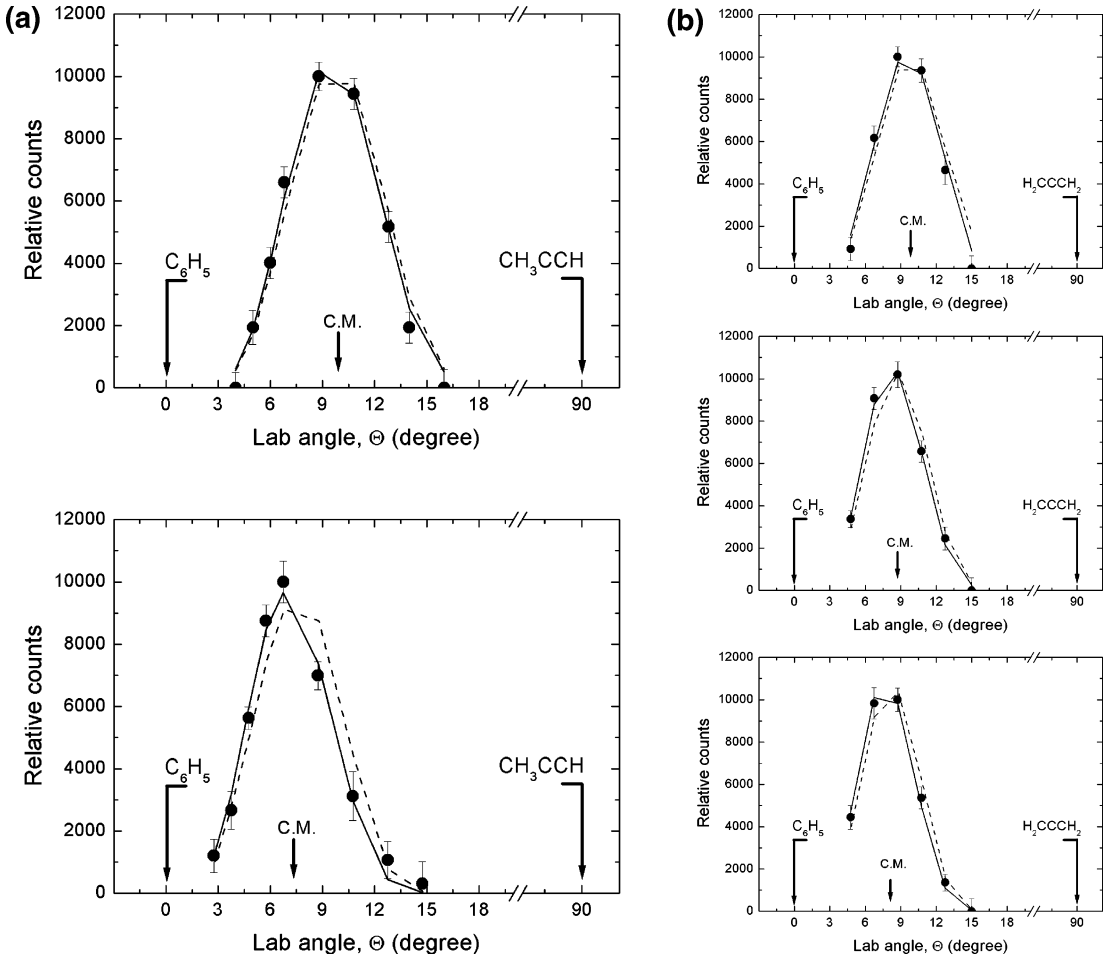

Figure 3. (a) Laboratory angular distributions of ion counts recorded at m/z 116 ($C_9H_8^+$) in the reaction of phenyl radicals with methylacetylene for two collision energies of 91.4 (upper) and 161.1 kJ mol^{-1} (lower). The circles are the experimental data, and the solid lines are the fits; dashed lines are shown for comparison for fits with isotropic CM angular distributions. C.M. defines the center-of-mass angle. (b) Laboratory angular distributions of ion counts recorded at m/z 116 ($C_9H_8^+$) in the reaction of phenyl radicals with allene for three collision energies of 92.7 (upper row), 117.4 (center row), and 132.1 kJ mol^{-1} (lower row). The circles are the experimental data, and the solid lines are the fits; dashed lines are shown for comparison for fits with isotropic CM angular distributions. CM defines the center-of-mass angle.

the shape of the center-of-mass angular distribution and the absent flux in the range of 155−180° suggest that at these conditions, the dynamics are likely at the borderline between an indirect and a direct reaction mechanism. Here, the reaction may involve a highly rovibrationally excited collision complex in a very shallow potential energy well. We would like to emphasize that despite the unfavorable kinematics of the reaction and the relative small velocity of the C_9H_8 reaction product of less than 160 ms^{-1} (which translates into a small Newton circle), the data obtained within the error limits from the T(θ) distribution depict unequivocally that the center-of-mass angular distributions are forward scattered with respect to the phenyl radical beam. No acceptable fit could be obtained with forward−backward symmetric and/or isotropic distributions. We also included an energy-dependence in our fitting routine (Section 2). Different threshold energies to the reaction of 10 and 45 kJ mol^{-1} are insensitive to the fit.

4. Discussion

4.1. Energetical Considerations. On the basis of the energetics of the reactions, we are attempting now to elucidate on the nature of the product isomer(s) formed in the reactions of phenyl radicals with methylacetylene and allene, respectively. Recall that the center-of-mass translational energy distributions suggest that the reactions are exoergic by a maximum of 13 kJ mol^{-1} (methylacetylene) (or even slightly endoergic by a few kJ mol^{-1}) and 16 ± 8 kJ mol^{-1} (allene). We can compare these data with theoretically expected reaction energies (Figure 6). Considering the phenyl−allene reaction, the experimental data are in excellent agreement with the formation of the 1-phenylallene isomer [$C_6H_5HCCCH_2$]. Even within the error limits, the formation of the 3-phenylmethylacetylene isomer [$C_6H_5CH_2$-CCH] (Figure 6), which is endoergic by about 19 kJ mol^{-1}, can be ruled out. At the present stage, however, a minor contribution of this isomer cannot be excluded (see discussion below). In the case of the phenyl−methylacetylene reaction, the reaction energies can account for the synthesis of both the 1-phenylmethylacetylene [$C_6H_5CCCH_3$] as well as the 1-phenylallene isomer [$C_6H_5HCCCH_2$] isomer. The difference in the reaction energies of only 6 kJ mol^{-1} is within the error limits of our experimental results. However, recalling that the reactions of phenyl with D4-methylacetylene (CD_3CCD) and D3-methylacetylene (CD_3CCH) depict the sole existence of atomic deuterium and atomic hydrogen elimination pathways, respectively (Section 3.1 and ref 9), we can deduce that in the corresponding phenyl−methylacetylene system, the hydrogen atom is only emitted from the acetylenic carbon atom. This leads us to the conclusion that the 1-phenylmethylacetylene molecule [$C_6H_5CCCH_3$] is the sole product in the reaction of phenyl radicals with methylacetylene. It should be stressed that in the

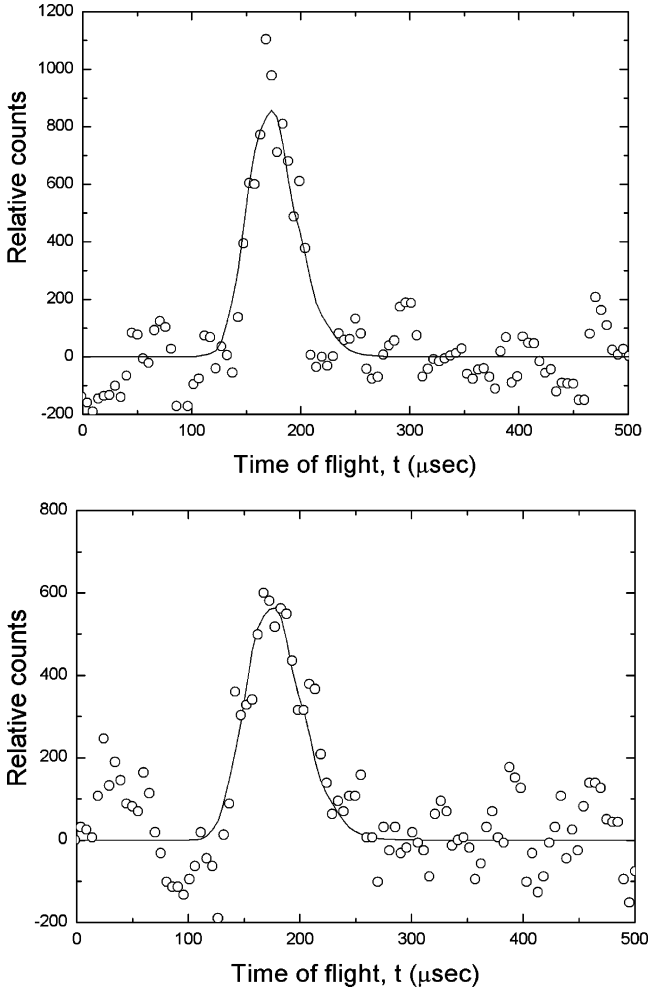

Figure 4. Time-of-flight spectra of m/z 119 ($C_9H_5D_3^+$) recorded during the reactions of phenyl radicals with D4-methylacetylene (upper) and D4-allene (lower) at the corresponding center of mass angles. The open circles are the experimental data, and the solid lines are the fits.

present range of collision energies, the formation of the indene isomer can be clearly rules out: here, we would expect reaction energies of −109 and −116 kJ mol^{-1} for the phenyl−methylacetylene and phenyl−allene systems, respectively. Likewise, an alternative reaction channel, which may result in an acetylenic hydrogen loss to form phenylmethylcarbene [$CH_3C_6H_5$-CC], is endoergic by about 209 kJ mol^{-1} and, hence, is energetically not accessible even at our highest collision energy of 161.1 kJ mol^{-1}.[9]

4.2. Proposed Reaction Dynamics.

4.2.1. Phenyl−Methylacetylene Reaction. In this section, we would like to combine the experimental results as discussed above and propose the most likely reaction dynamics in the phenyl−methylacetylene and phenyl−allene systems. Let us start with the reaction of phenyl radicals with methylacetylene. To correlate the structure of the 1-phenylmethylacetylene reaction product [$C_6H_5CCCH_3$] with the reactants, we propose that the phenyl radical adds with its radical center to the α-carbon of the methylacetylene reactant.[19] Two effects can direct the attack to the α position. First, the sterical hindrance of the methyl group reduces the cone of acceptance of an addition of the phenyl radical to the β-carbon atom. Second, the phenyl radical must be classified, due to the unpaired electron, as an electron-deficient species. Therefore, the attack is preferentially directed to the carbon atom of the methylacetylene molecule holding the highest negative charge. Here, the α-carbon has a charge of −0.26 compared to +0.14 of the β-carbon atom.[20] Also, a recent theoretical work on this reaction suggested that the addition of the phenyl radical to the α-carbon atom has a lower barrier (12.6 kJ mol^{-1}) compared to an addition to the central carbon atom (18.1 kJ mol^{-1}).[21] Therefore, the sterical effect, the enhanced negative charge density, and the lower entrance barrier likely direct the addition of the phenyl radical to the α-carbon atom of methylacetylene. Recall that a preferential site-specific radical attack was observed previously in the crossed beam reactions of methylacetylene with CN radicals,[22] C_2D radicals,[23] and $C(^3P_j)$ as well.[24] The addition of the phenyl radical to the α position leads to the C_9H_9 reaction intermediate i1 via indirect scattering dynamics; the complex-forming reaction dynamics have been inferred from the center-of-mass angular distributions, too. This intermediate resides in a very shallow potential energy well of only 152 kJ mol^{-1} (Figure 6) and can isomerize easily to its trans form (i2). Both the cis and the trans isomers can undergo unimolecular decomposition via atomic hydrogen loss pathways involving a tight exit transition state; computations suggest that the transition state resides 14 kJ mol^{-1} above the separated product molecules. The tight exit transition state has been verified in our experiments based on the off-zero peaking of the center-of-mass translational energy distributions. On the basis of the energy-dependence of the cross section (Section 2), the experiments indicated threshold energies to the reaction, E_o, ranging between 10 and 45 kJ mol^{-1}. This order of magnitude agrees nicely with the computed entrance barrier to addition of 19 kJ mol^{-1} (Figure 6). Also, it is important to address briefly the nondetection of the methyl group loss. This pathway would require an addition of the phenyl radical to the β-carbon atom. However, the latter addition pathway has been shown to be unfavorable due to the screening of this position by the methyl group and the unfavorable charge density of this position (see above). This can explain the nonexistence of the phenyl versus methyl exchange channel at least over the range of collision energies investigated in the present study.

Finally, it is important to address the collision energy-dependence of the reaction dynamics. As evident from the center-of-mass angular distributions and the enhanced forward-scattering with increasing collision energy, the life times of the reaction intermediates i1/i2 decrease as the collision energy increases. Having proposed the formation of the i1/i2 intermediates, which decompose to form the 1−phenylmethylacetylene reaction product [$C_6H_5CCCH_3$], we attempt now to estimate the life time of i1/i2. Recall that at the collision energies investigated, the intermediates can be classified, within the error limits, as osculation complexes.[17] Here, the rotational period of the complex acts as a clock in the molecular beam experiment and can be utilized to estimate the lifetime τ of the decomposing complex. The osculating complex model relates the intensity ratio of $T(\theta)$ at both poles to τ via eqs 1 and 2 where t_{rot} represents the rotational period of the complex.

$$I(180^0)/I(0^0) = \exp\left(-\frac{t_{rot}}{2\tau}\right) \quad (1)$$

$$t_{rot} = 2\pi I_i/L_{max} \quad (2)$$

I_i represents the moment of inertia of the complex rotating around the i-axis (i = A, B, C), and L_{max} represents the maximum orbital angular momentum. Using the ab initio geometries of the cis/trans intermediates *i*1/*i*2,[9] we can compute the moments of inertia (Table 2). Taking the maximum impact

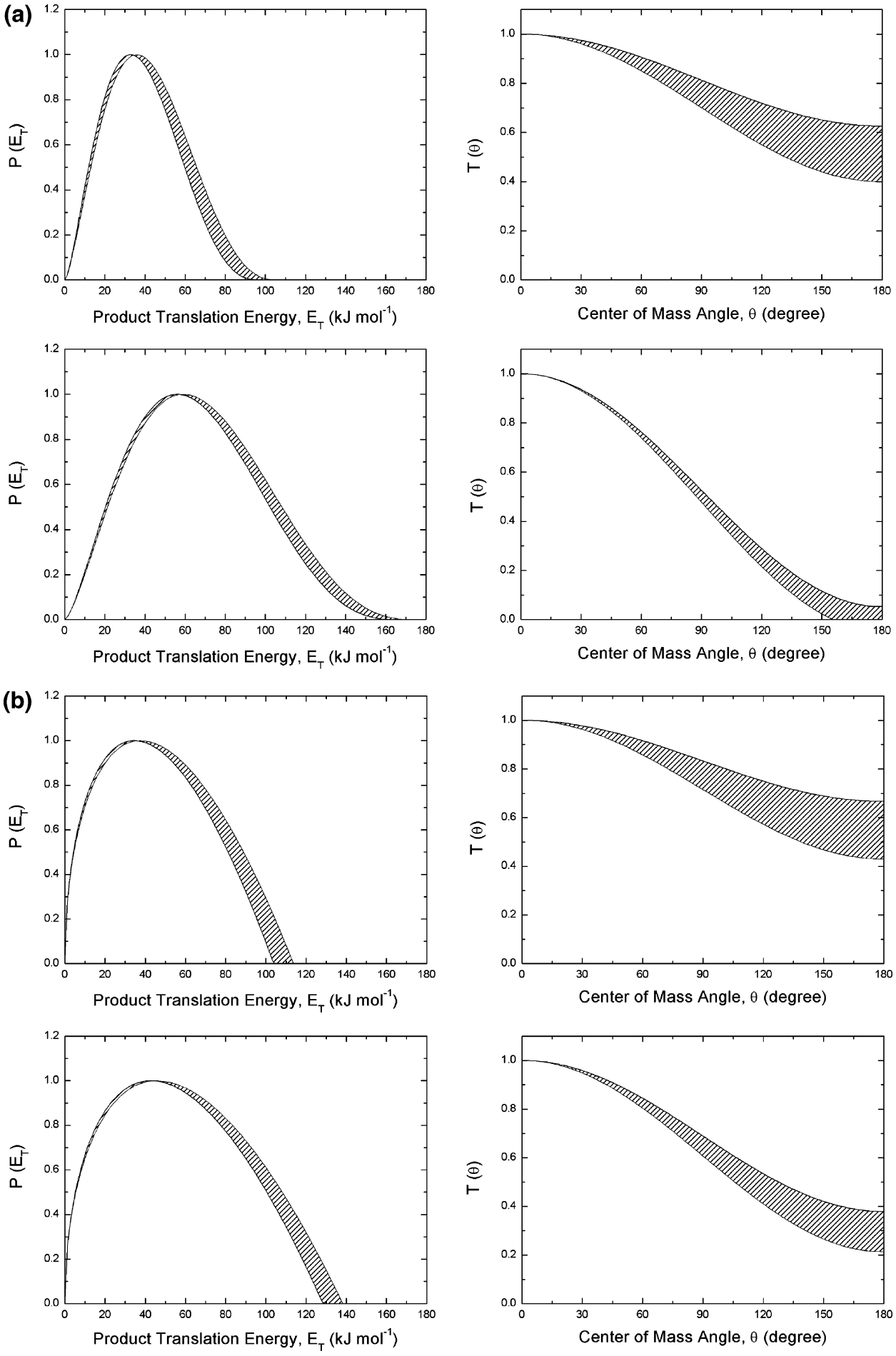
(a)
P (E_T)
Product Translation Energy, E_T (kJ mol^-1)
T (θ)
Center of Mass Angle, θ (degree)
P (E_T)
Product Translation Energy, E_T (kJ mol^-1)
T (θ)
Center of Mass Angle, θ (degree)
(b)
P (E_T)
Product Translation Energy, E_T (kJ mol^-1)
T (θ)
Center of Mass Angle, θ (degree)
P (E_T)
Product Translation Energy, E_T (kJ mol^-1)
T (θ)
Center of Mass Angle, θ (degree)

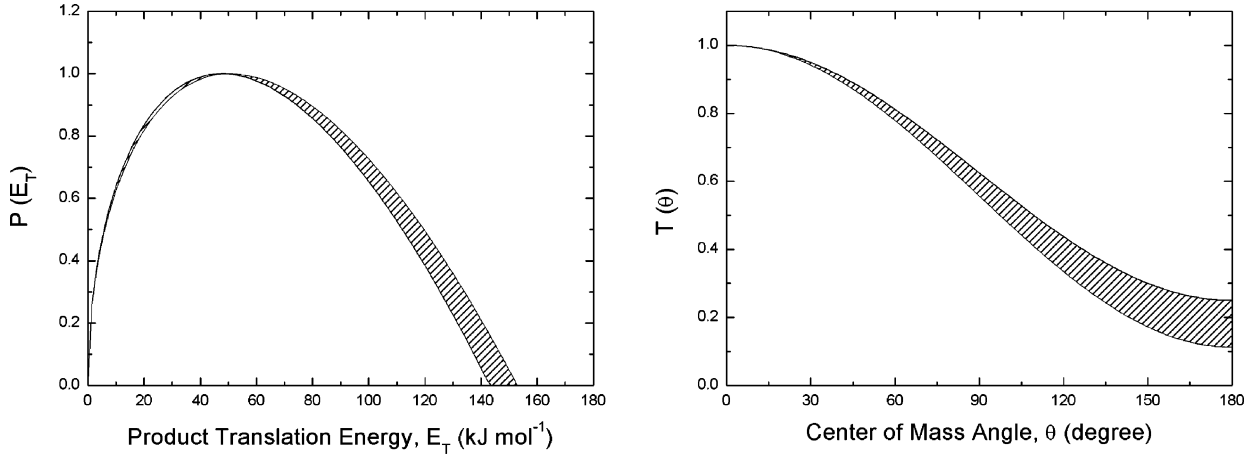

Figure 5. (a) Center-of-mass translational (left column) and angular (distributions (right column) of the C_9H_8 product formed in the reaction of phenyl radicals with methylacetylene at two collision energies of 91.4 (upper row) and 161.1 kJ mol^{-1} (lower row). The hatched areas account for the experimental error limits of the laboratory angular distributions (Figure 2a) as well as peak velocities and speed ratios (Table 1). (b) Center-of-mass translational (left column) and angular distributions (right column) of the C_9H_8 product formed in the reaction of phenyl radicals with allene at three collision energies 92.7 (upper row), 117.4 (center row), and 132.1 kJ mol^{-1} (lower row). The hatched areas account for the experimental error limits of the laboratory angular distributions (Figure 2b) as well as peak velocities and speed ratios (Table 1).

parameter to be in the order of 2.4 Å estimated from the structure of the transition state in the entrance channel, the reduced mass of the reactants, and the relative velocity of the reactants, maximum orbital angular momenta of 27×10^{-33} kg m^2 s^{-1} ($E_c = 91.4$ kJ mol^{-1}) and 35×10^{-33} kg m^2 s^{-1} ($E_c = 161.1$ kJ mol^{-1}) are obtained. Table 2 summarized the results. We can compare the estimated lifetimes with the lifetimes of decomposing complexes in related reactions of carbon atoms with unsaturated hydrocarbons.[16] The absolute value of τ depends on the rotation axis, i.e., B, C vs A. Even at the lower collision energy, we can conclude that the order of the life times of the complexes is lower than the time necessary for a complete energy randomization in the intermediate to occur (recall that we were not able to detect the hydrogen loss pathway in the reaction of phenyl radicals with D3-methylacetylene).

These findings can be compared now to the fraction of the total available energy, i.e., the sum of the reaction energy plus the collision energy, released into the translational degrees of freedom of the reaction products. Here, fractions of 40−45% indicate that the reaction proceeds on a rather short time scale via short-lived intermediates. As evident from the failed detection of the indene isomer, which would require multiple isomerization steps via hydrogen shifts and ring closures, the life time of the reaction intermediates *i*1/*i*2 is too short for any of the isomerization processes required in the synthesis of indene to proceed. Likewise, these results show that lifetimes of *i*1/*i*2 are too short to allow an energy "flow" from the position of the initial carbon−carbon single bond formation to the terminal carbon-hydrogen bond; as verified experimentally, this hinders the formation of the 1-phenylallene isomer [$C_6H_5HCCCH_2$].

4.2.2. Phenyl−Allene Reaction. Similar to the reaction of methylacetylene with phenyl, the reaction dynamics in the phenyl−allene system were inferred to be indirect (Section 3.2) and found to proceed via a C_9H_9 reaction intermediate. Here, the phenyl radical can add to the terminal carbon atom via an entrance barrier of about 15 kJ mol^{-1} leading to a weekly bound (−143 kJ mol^{-1}) reaction complex. In allene, the central carbon atom has a charge of + 0.53; the terminal carbon atoms hold charges of −0.61.[25] Since the phenyl radical is categorized as an electron-deficient reactant, we expect a preferential addition to the terminal carbon atom of the allene molecule leading to a $C_6H_5H_2CCCH$ intermediate (*i*1) (Figure 6). Note that in a related, indirect reaction of cyano radicals with allene,[20] the cyano radical was found to add solely to the terminal carbon atom of allene, too. On the basis of the overall energetics of the reaction, intermediate *i*1 was found to decompose at least to the 1-phenylallene isomer [$C_6H_5HCCCH_2$]. This process involves a tight exit transition state as verified in our experiments (center-of-mass translational energy distributions, Section 3.2) and by previous electronic structure calculations (Figure 6). On the basis of the geometries of the reactants and products, an initial addition of the phenyl radical to the central allene carbon atom can likely be ruled out. This conclusion also yields support from a recent theoretical investigation of the relative importance of the entrance channels of addition of the phenyl radical to the central versus one of the terminal carbon atoms.[4] Here, Park et al. suggested that phenyl radicals add exclusively to the terminal carbon atom of the allene molecule.

How can the dynamics account for the preferential formation of the 1-phenylallene isomer [$C_6H_5HCCCH_2$] and the, at most, minor importance of the 3-phenylmethylacetylene isomer [C_6H_5-CH_2CCH] (Figure 6)? On the basis of the computed potential energy surface, intermediate *i*3 resides in a very shallow potential energy well of only 143 kJ mol^{-1}. As evident from the center-of-mass angular distributions and the pronounced forward-scattering with rising collision energy, the lifetimes of the *i*3 intermediate decreases as the collision energy rises. Similar to the methylacetylene−phenyl system, we can estimate the lifetime of the reaction intermediates based on the osculating complex model (eqs 1 and 2). Using the ab initio geometries of intermediate *i*3, we can compute the moments of inertia (Table 3). Taking the maximum impact parameter to be in the order of 2.3 Å estimated from the structure of the transition state in the entrance channel, the reduced mass of the reactants, and the relative velocity of the reactants, maximum orbital angular momenta of 27×10^{-33} kg m^2 s^{-1} ($E_c = 92.7$ kJ mol^{-1}), 30×10^{-33} kg m^2 s^{-1} ($E_c = 117.4$ kJ mol^{-1}), and 32×10^{-33} kg m^2 s^{-1} ($E_c = 132.1$ kJ mol^{-1}) are computed. The life times of the intermediate are in the same order compared to intermediates *i*1/*i*2 in the phenyl−methylacetylene system. Having established that the energy randomization in *i*1/*i*2 is likely incomplete, we can propose that due to the similar lifetimes of the reaction intermediates *i*1/*i*2 versus *i*3, the energy randomization in *i*3 is likely to be incomplete, too, before the decomposition of intermediate *i*3 occurs. Since the initial localization of the energy in the newly formed carbon−carbon

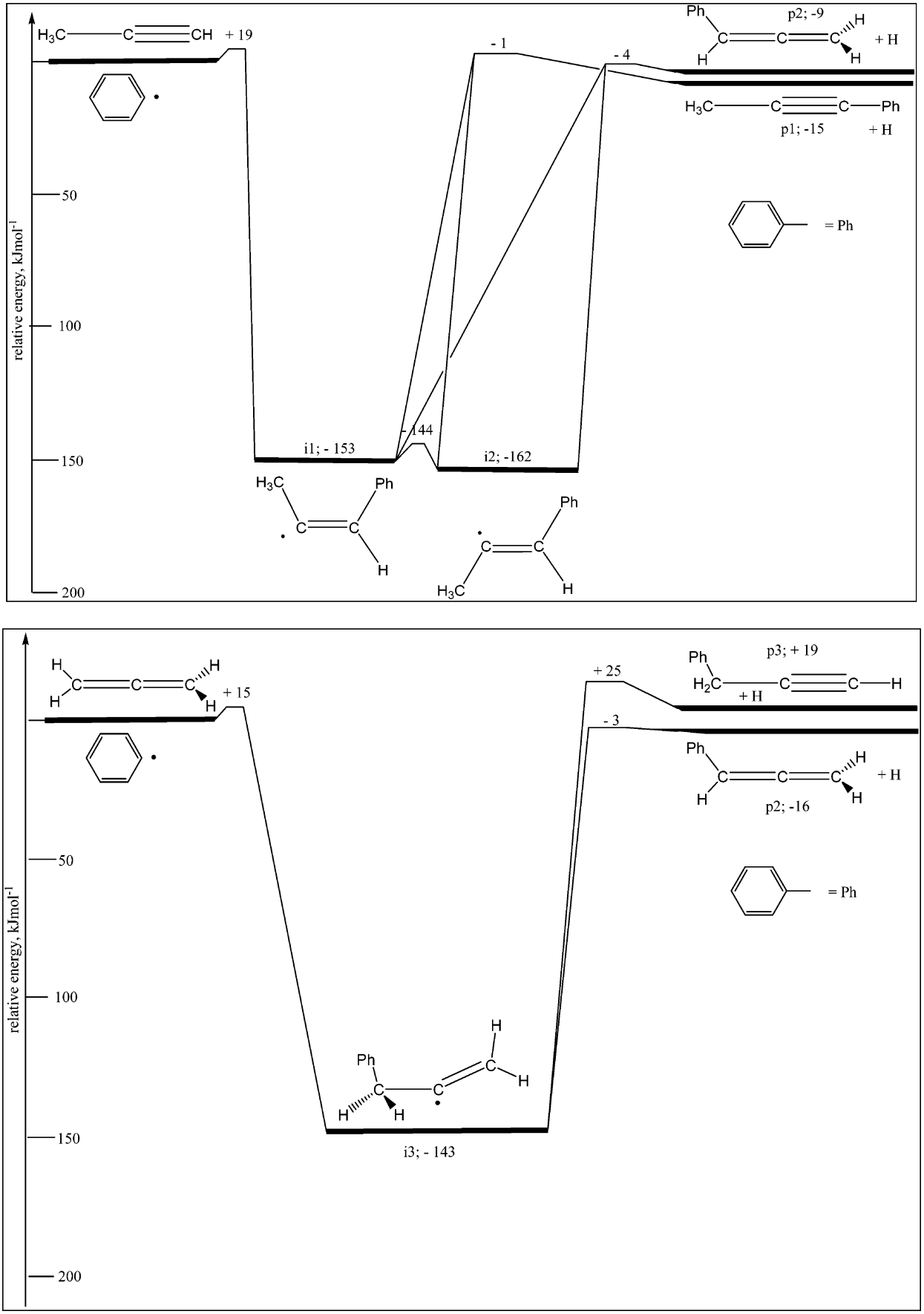

Figure 6. Relevant stationary points of the C_9H_9 PES involved in the reaction of phenyl radicals with methylacetylene (upper) and allene (lower). Data are compiled from ref 7.

bond, it is more likely that the adjacent hydrogen atom is emitted to form the 1-phenylallene molecule than an "energy flow" over three bonds to the terminal carbon−hydrogen bond leading to the 3-phenylmethylacetylene isomer [$C_6H_5CH_2CCH$]. Therefore,

TABLE 2: Moments of Inertia, Rotational Times, and Estimated Life Times of the *i*1/*i*2 Intermediates

	I_A (kg m^2)	I_B (kg m^2)	I_C (kg m^2)
*i*1	2.1×10^{-45}	8.0×10^{-45}	9.9×10^{-45}
*i*2	1.7×10^{-45}	9.6×10^{-45}	11.2×10^{-45}
$E_c = 91.4$ kJ mol^{-1}	t_{rot}(A) (ps)	t_{rot}(B) (ps)	t_{rot}(C) (ps)
*i*1	0.5	1.9	2.3
*i*2	0.4	2.2	2.6
$E_c = 161.1$ kJ mol^{-1}	t_{rot}(A) (ps)	t_{rot}(B) (ps)	t_{rot}(C) (ps)
*i*1	0.4	1.4	1.8
*i*2	0.3	1.7	2.0
$E_c = 91.4$ kJ mol^{-1}	τ(A) (ps)	τ(B) (ps)	τ(C) (ps)
*i*1	0.3 ± 0.1	1.1 ± 0.3	1.4 ± 0.4
*i*2	0.2 ± 0.1	1.3 ± 0.4	1.5 ± 0.5
$E_c = 161.1$ kJ mol^{-1}	τ(A) (ps)	τ(B) (ps)	τ(C) (ps)
*i*1	< 0.1	< 0.3	< 0.3
*i*2	< 0.1	< 0.3	< 0.3

TABLE 3: Moments of Inertia, Rotational Times, and Estimated Life Times of the *i*3 Intermediate at Three Collision Energies Investigated in the Present Study

	I_A (kg m^2)	I_B (kg m^2)	I_C (kg m^2)
*i*3	2.5×10^{-45}	7.6×10^{-45}	8.1×10^{-45}
	t_{rot}(A) (ps)	t_{rot}(B) (ps)	t_{rot}(C) (ps)
$E_c = 92.9$ kJ mol^{-1}	0.6	1.8	1.9
$E_c = 117.4$ kJ mol^{-1}	0.5	1.6	1.7
$E_c = 132.1$ kJ mol^{-1}	0.5	1.5	1.6
	τ(A) (ps)	τ(B) (ps)	τ(C) (ps)
$E_c = 92.9$ kJ mol^{-1}	0.5 ± 0.1	1.5 ± 0.4	1.6 ± 0.5
$E_c = 117.4$ kJ mol^{-1}	0.2 ± 0.1	0.7 ± 0.3	0.7 ± 0.3
$E_c = 132.1$ kJ mol^{-1}	0.1 ± 0.05	0.4 ± 0.1	0.5 ± 0.1

the reaction energies, the time scale of the reaction, and the incomplete energy randomization in the decomposing intermediate *i*3 would suggest the formation of the 1-phenylallene isomer [$C_6H_5HCCCH_2$]. Note that similar to the phenyl−methylacetylene system, fractions of the total available energy channeling into the translational degrees of the reaction products of 42−48% also indicate that the time scale of the reaction is rather short.

5. Conclusions and Summary

The reactions of phenyl radicals with methylacetylene and allene and their perdeuterated counterparts were investigated under single collision conditions at various collision energies utilizing a crossed molecular beam machine. Over this range of collision energies, both reactions share common features. The reactions are indirect and proceed via addition of the phenyl radical with its unpaired electron to the terminal carbon atom of the methylacetylene and allene reactants leading to doublet radical intermediates *i*1 and *i*3, respectively (Figure 6); *i*1 can isomerize to *i*2. All intermediates reside in relatively shallow potential energy wells located 143−162 kJ mol^{-1} below the separated reactant molecules. On the basis of the collision energy-dependence of the center-of-mass angular distributions and the single channel fits of each reaction system, the life times of these intermediates are shorter than their rotation periods. Detailed studies with isotopically labeled reactants and the information on the energetics of the reactions show that the energy randomization in *i*1, *i*2, and *i*3 prior to their decomposition is incomplete. These intermediates undergo atomic hydrogen losses via tight exit transition states leading to the 1-phenylmethylacetylene isomer [$CH_3CCC_6H_5$] and 1-phenylallene isomer [$C_6H_5HCCCH_2$] in the methylacetylene and allene systems, respectively. Also, we were able to derive upper limits of 5% of the methyl group loss channel in the phenyl−methylacetylene reaction. We recognize that our experimental approach cannot detect the $PhCH_2 + C_2H_2$ (up to 18%) as predicted for the phenyl−allene system. Here, dissociative ionization of the C_9H_8 reaction products prevent an identification of a potential $PhCH_2$ product. Nevertheless, the identification of two C_9H_8 isomers formed via the phenyl versus atomic hydrogen exchange pathways suggests that similar processes can also form these molecules in combustion flames and in circumstellar envelopes of dying carbon stars such as IRC+10216 or planetary nebulae. Here, 1-phenylmethylacetylene and 1-phenylallene may act as precursors to (methyl) substituted polycyclic aromatic hydrocarbons (PAHs) in successive reactions.

Acknowledgment. This work was supported by the U.S. Department of Energy, Basic Energy Sciences (DE-FG02-03ER15411). We also thank Ed Kawamura (University of Hawaii, Department of Chemistry) for assistance.

References and Notes

(1) Appel, J.; Bockhron, H.; Frenklach, M. *Combust. Flame* **2000**, *121*, 122. Richter, H.; Howard, J. B. *Phys. Chem. Chem. Phys.* **2002**, *4*, 2038.
(2) Kazakov, A.; Frenklach, M. *Combust. Flame* **1998**, *112*, 270.
(3) Frenklach, M.; Feigelson, E. D. *Astrophys. J.* **1989**, *341*, 372.
(4) (a) Park, J.; Tokmakov, I. V.; Lin, M. C. *J. Phys. Chem. A* **2007**, 10.1021/jp0708502. (b) Choi, Y. M.; Park, J.; Lin, M. C. *Chem. Phys. Chem.* **2004**, *5*, 661. (c) Choi, Y. M.; Park, J.; Lin, M. C. *J. Phys. Chem. A* **2003**, *107*, 7755. (d) Choi, Y. M.; Xia, W. S.; Park, J.; Lin, M. C. *J. Phys. Chem. A* **2000**, *104*, 7030. (e) Nam, G.-J.; Xia, W.; Park, J.; Lin, M. C. *J. Phys. Chem. A* **2000**, *104*, 1233.
(5) Vereecken, L.; Bettinger, H. F.; Peeters, J. *Phys. Chem. Chem. Phys.* **2002**, *4*, 2019.
(6) Vereecken, L.; Peeters, J.; Bettinger, H. F.; Kaiser, R. I.; Schleyer, P. v. P.; Schaefer, H. F., III. *J. Am. Chem. Soc.* **2002**, *124*, 2781.
(7) Vereecken, L.; Peeters, J. *Phys. Chem. Chem. Phys.* **2003**, *5*, 2807.
(8) Kaiser, R. I.; Vereecken, L.; Peeters, J.; Bettinger, H. F.; Schleyer, P. v. R.; Schaefer, H. F., III. *Astron. Astrophys.* **2003**, *406*, 385.
(9) Kaiser, R. I.; Asvany, O.; Lee, Y. T.; Bettinger, H. F.; Schleyer, P. v. P.; Schaefer, H. F., III. *J. Chem. Phys.* **2000**, *112*, 4994.
(10) Hahndorf, I.; Lee, Y. T.; Kaiser, R. I.; Vereecken, L.; Peeters, J.; Bettinger, H. F.; Schleyer, P.v.R.; Schaefer, H. F., III *J. Chem. Phys.* **2002**, *116*, 3248.
(11) Balucani, N.; Lee, H. Y.; Mebel, A.; Lee, Y. T.; Kaiser, R. I. *J. Chem. Phys.* **2001**, *115*, 5107.
(12) (a) Gu, X.; Guo, Y.; Kawamura, E.; Kaiser, R. I. *J. Vac. Sci. Technol. A* **2006**, *24*, 505. (b) Guo, Y.; Gu, X.; Kaiser, R. I. *Int. Mass J. Spec.* **2006**, *249−250*, 420.
(13) Stranges, D.; Stemmler, M.; Yang, X.; Chesko, J. D.; Suits, A. G.; Lee, Y. T. *J. Chem. Phys.* **1998**, *109*, 5372.
(14) Kohn, D. W.; Clauberg, H.; Chen, P. *Rev. Sci. Instr.* **1992**, *63*, 4003.
(15) (a) Weiss, M. S. Ph.D. Thesis, University of California, Berkeley, 1986. (b) Vernon, M. Ph.D. Thesis, University of California, Berkeley, 1981. (c) Kaiser, R. I.; Mebel, A. M.; Balucani, N.; Lee, Y. T.; Stahl, F.; Schleyer, P. v. R.; Schaefer, H. F. *Faraday Discuss.* 2001, *119*, 51.
(16) Levine, R. D. *Molecular Reaction Dynamics*; Cambridge University Press: Cambridge, 2005.
(17) (a) Kaiser, R. I. *Chem. Rev.* **2002**, *102*, 1309. (b) Kaiser, R. I.; Mebel, A. M. *Int. Rev. Physical Chemistry* **2002**, *21*, 307.
(18) Miller, W. B.; Safron, S. A.; Herschbach, D. R. *Discuss. Faraday. Society* **1967**, *44*, 108, 291.
(19) The alpha carbon atom is defined as the carbon atom holding the acetylenic hydrogen atom.
(20) Mebel, A. M. Unpublished results, 2007.
(21) Tokmakov, I. V.; Joonbum Park, J.; Lin, M. C. *Chem. Phys. Chem.* **2005**, *6*, 2075.
(22) Balucani, N.; Kaiser, R. I.; Osamura, Y. *J. Phys. Chem. A* **2002**, *106*, 4301.
(23) Kaiser, R. I.; Chiong, C. C.; Asvany, O.; Lee, Y. T.; Stahl, F.; Schleyer, P. v. R.; Schaefer, H. F. *J. Chem. Phys.* **2001**, *114*, 3488.
(24) Kaiser, R. I.; Stranges, D.; Lee, Y. T.; Suits, A. G. *J. Chem. Phys.* **1996**, *105*, 8721.
(25) Kaiser, R. I.; Mebel, A. M.; Chang, A. H. H.; Lin, S. H.; Lee, Y. T. *J. Chem. Phys.* **1999**, *110*, 10330.